

Mesoporous polystyrene nanoparticles synthesized by semicontinuous heterophase polymerization

O. Esquivel · M. E. Treviño · H. Saade · J. E. Puig ·
E. Mendizábal · R. G. López

Received: 4 March 2010 / Revised: 5 August 2010 / Accepted: 18 August 2010 /
Published online: 26 August 2010
© Springer-Verlag 2010

Abstract The synthesis by semicontinuous heterophase polymerization and the characterization of mesoporous crosslinked polystyrene particles in the nanometer range (ca. 30 nm) are reported here. The particles have pores between 6 and 8 nm in diameter and pore volume around 0.40 cm³/g. In spite that the polymerization was not carried out at highly monomer-starved conditions, particles with narrow size distribution were obtained, which is ascribed to inter-particle hetero-coagulation at latter stages of polymerization, due to lack of enough surfactant to cover all the particles even before 45% global conversion.

Keywords Semicontinuous heterophase polymerization · Mesoporous polystyrene nanoparticles · Radical polymerization

Introduction

Polystyrene, polyacrylamides, and polymethacrylates porous microparticles have been used in applications such as chromatography, catalysis, ion-exchange, solid-phase synthesis, enzyme and cell immobilization [1, 2], and drug delivery systems [3–5]. For the later application, composites of magnetic particles–polymer microparticles with drugs chemically attached to their surface are currently being investigated [4–7]. An interesting option for preparing this type of composites is synthesizing porous microparticles containing magnetic nanoparticles inside their

O. Esquivel · M. E. Treviño · H. Saade · R. G. López (✉)
Departamento de Procesos de Polimerización, Centro de Investigación en Química Aplicada,
Blvd. E. Reyna # 140, 25253 Saltillo, COAH, Mexico
e-mail: glopez@ciqa.mx

J. E. Puig · E. Mendizábal
Departamentos de Química e Ingeniería Química, CUCEI, Universidad de Guadalajara,
Blvd. M. García-Barragán # 1451, 44430 Guadalajara, JAL, Mexico

pores [4]. Porous microparticles with typical sizes ranging from some tenths of micrometer to micrometers are usually prepared by emulsion polymerization [2, 8–10] and up to millimeters by suspension polymerization [1, 11]. Usually, these two techniques involve the polymerization of a monomer and a crosslinking agent in the presence of a porogen. The porogen is a monomer diluent used to form the pores during the polymerization. Toluene, chlorobenzene, *n*-dodecane, and carbon tetrachloride are common porogens for styrene [12]. The crosslinking agent, such as divinylbenzene (DVB) for styrene, is needed to harden the particles and make the polymer chains insoluble in the porogen [13]. The combined effects of the porogen and the crosslinking agent determine the porosity and the pore size [13], rendering pore volumes up to 1.2 cm³/g [1, 2, 11] and pore diameters in the range of ca. 10 nm to 1 μm [14].

Several studies on porous polymeric microparticles for drug delivery systems [4–7] indicate that mesoporous (2–50 nm in pore diameter) polymeric nanoparticles with diameters <100 nm are more effective as carriers mainly because of their size, they are able to circumvent the body's defense system. Because of the intrinsic characteristics of suspension and emulsion polymerization, these processes are not suitable for the systematic synthesis of mesoporous nanoparticles. Techniques allowing the synthesis of polymer particles in the nanometer range are microemulsion polymerization [15, 16] and a recently reported technique named semicontinuous heterophase polymerization [17, 18], which is capable of producing polymeric nanoparticles from 20 to 50 nm with surfactant contents much lower than those required in microemulsion polymerization. In spite of this, as far as we know, there are no reports on the synthesis of porous polymeric nanoparticles by any of these techniques.

Here, the synthesis of mesoporous polystyrene nanoparticles with average diameters <50 nm by semicontinuous heterophase polymerization is reported. Average particle sizes, particle size distribution, pore volume, and average pore diameter, were determined. This is the first report on synthesis by semicontinuous heterophase polymerization and the characterization of mesoporous polymeric nanoparticles with average diameters <50 nm.

Experimental section

Styrene (St), 99% pure from Sigma-Aldrich, reagent-grade DVB from Sigma-Aldrich, and toluene, 99.9% pure from J.T. Baker, were distilled under reduced pressure and stored at 4 °C. Sodium dodecylsulfate (SDS), 98.5% pure, and ammonium persulfate (APS), 98% pure, both from Sigma-Aldrich, were used as received. De-ionized and triple-distilled water was drawn from a Millipore system.

Polymerizations with identical composition, procedure, and feeding rate were carried out at 60 °C in a 150-mL jacketed glass reactor equipped with a reflux condenser and inlets for argon, monomer feed, mechanical agitation (450 rpm), and sampling. A 45°-pitched down flow four-bladed impeller was used. The procedure was as follows: 4.3 g of SDS and 0.017 g of APS were dissolved in 91.3 g of water and charged into the reactor. This solution was bubbled with argon for 1 h at room

temperature, heated to 60 °C and then, the organic mixture (17.5 g of St, 11.8 g of toluene, and 4.4 g of DVB) was fed at a rate of 0.094 g/min using a KD Scientific syringe pump. After the addition of the organic mixture was completed (6 h), the reaction was allowed to proceed for two more hours. Samples were withdrawn at given times to determine conversion gravimetrically, particle size, particle size distribution, porosity, and pore radius. From these samples, the surfactant, non-reacted monomers and toluene were eliminated from the latex by dialysis using a porous membrane (Sigma) with exclusion size corresponding to molar masses larger than 12,000 g/mol; dialysis was carried out for 2 weeks changing the fresh water twice a day using large volumes of water. The dialyzed dispersion was then subjected to liofilization to recover the polymer.

Particle size and polydispersity index (PDI) were determined in a JEOL JSM-7401F scanning-transmission electron microscope (STEM). For this, 0.01 g of latex was diluted in 10 g of water, and a drop of this dispersion was added to a copper grid, and allowed to dry. At least 1,000 particles were measured from the micrographs to obtain the PDI (D_w/D_n), being D_w and D_n the weight- and number-average diameters, respectively, which were calculated using the following equations:

$$D_n = \frac{\sum_i n_i D_i}{\sum_i n_i} = \frac{\sum n_i D_i}{n} \quad (1)$$

$$D_w = \frac{\sum_i n_i D_i^4}{\sum_i n_i D_i^3} \quad (2)$$

Here, n_i is the number of particles of size D_i and n is the total number of measured particles.

Pore volume (ϕ) and average pore radius (R_{pore}) were determined in an automated surface area and pore size analyzer Quantachrome Autosorb 1 MPR using the Quantachrome software and the density fluctuation theory (DFT) N_2 -adsorption–desorption isotherm, which allows the evaluation of the pore size distribution [19].

Results and discussion

The initially transparent surfactant solution becomes bluish upon monomer addition due to particle formation and increasingly opaque and more viscous with further monomer addition and with the progress of the reaction. The final latexes have remained stable after 6 months of storage.

Figure 1 depicts the instantaneous (x_i) and the global (X) conversions as a function of time (t) for two repetitive reactions. The instantaneous conversion is the fraction of added monomer up to time t that has changed into polymer, whereas the global conversion is the fraction of the total monomer added in the process that has polymerized at time t . Figure 1 reveals that x_i increases rapidly up to values ca. 60% in about 100 min, after which x_i increases more slowly to reach final conversions close to 80%. Global conversion increases almost linearly with time.

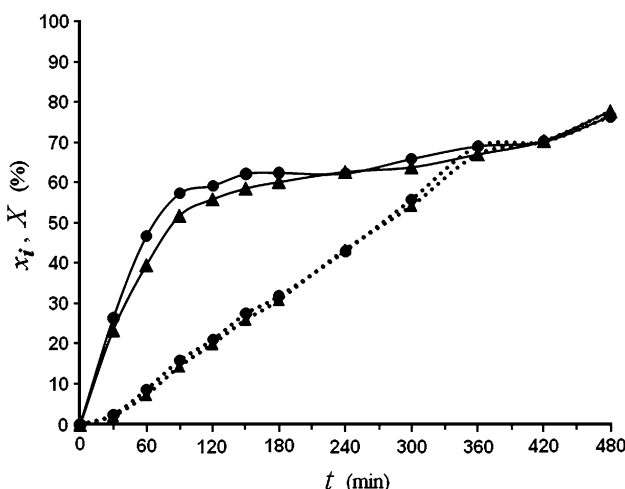


Fig. 1 Instantaneous, x_i (solid lines) and global conversion, X (dashed lines) as a function of time for run 1 (filled triangle), run 2 (filled circle)

The post-addition reaction yields only a small increment in conversion. Moreover, both runs exhibit nearly identical results. Relatively low values of x_i during the addition period indicate that in spite of the very low feeding rate of organic mixture, polymerizations were not carried out at highly monomer-starved conditions. The reason for this is that toluene acts as a monomer diluent, which slows down propagation reactions inside the particles.

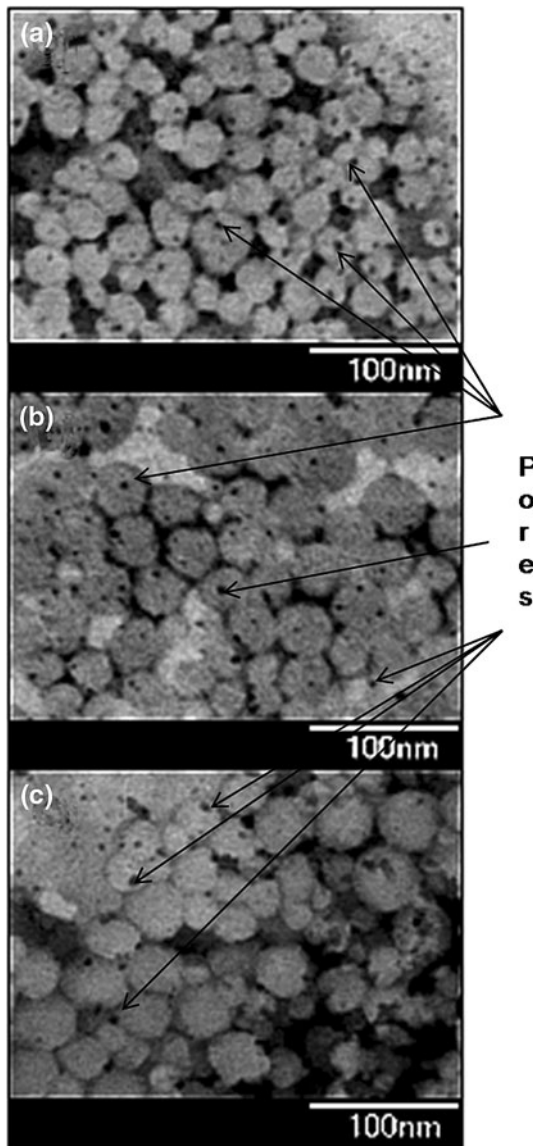
Figure 2 shows micrographs of the polystyrene nanoparticles obtained at different stages of the semicontinuous polymerization. These pictures show that particles are spherical with similar sizes and in the nanometer range. Close examination of these micrographs reveals the existence of small pores in the surface of these particles (see arrows in Fig. 2).

Figure 3 discloses the particle size histograms for the nanoparticles shown in Fig. 2. D_n and PDI are reported in Table 1. At low and medium conversions, the PDI is relatively narrow ($D_w/D_n \approx 1.2$) and becomes narrower ($D_w/D_n \approx 1.1$) at the end of reaction.

Figure 4 depicts D_n as a function of global conversion. This figure shows a continuous particle growth with conversion that goes from about 9 nm at 15% conversion to 29 nm at the maximum reached conversion (ca. 78%). Nevertheless, final particle sizes are in the nanometer range.

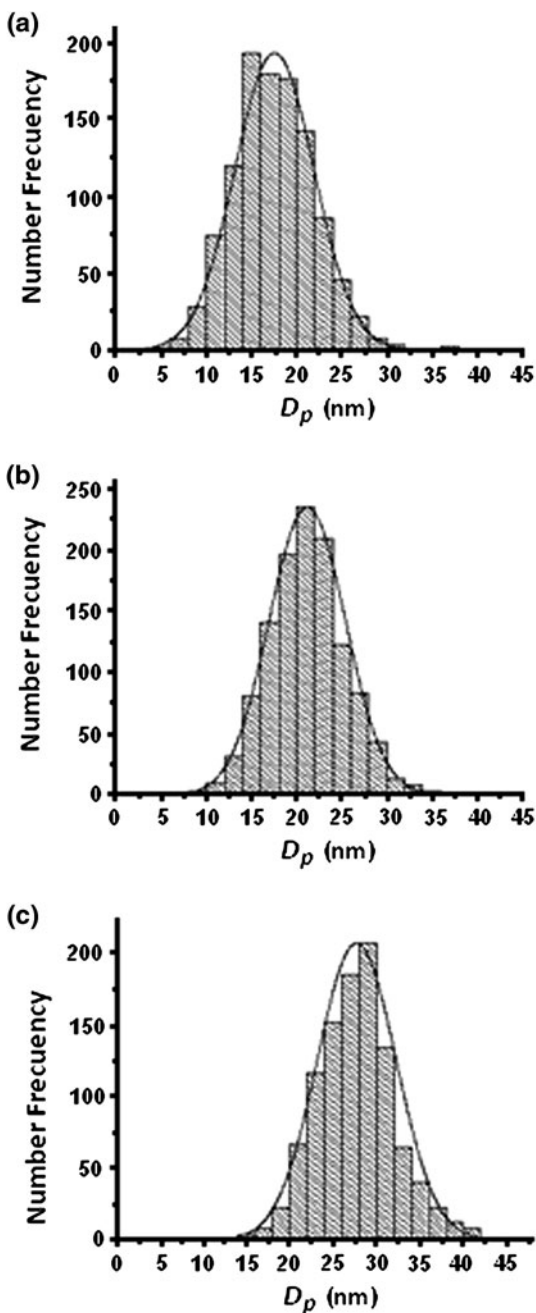
Table 2 reports average pore radius (R_{pore}) and average pore volume (ϕ) at low, intermediate, and high global conversions for the repetitive runs. Figure 5 reproduces the graph provided by the automated surface area and pore size analyzer for a polymer sample obtained at the end of the reaction. Data in Table 2 indicate good reproducibility, that the pore radius augments slightly as global conversion increases and that after 43.5% global conversion it remains practically constant at values on the order of 3.5–4.0 nm. The pore volume increases slightly from $0.32 \text{ cm}^3/\text{g}$ at low conversions to $0.42 \text{ cm}^3/\text{g}$ at intermediate conversions, and then it decreases slightly

Fig. 2 STEM micrographs at different global conversions in run 1: **a** 26.1%, **b** 43.5%, and **c** 77.9%



at higher conversions; however, this variation is within experimental error. Calculations based on the formulation in polymerizations, considering that the initial toluene concentration inside particles remains the same during polymerization, indicate that at 80% global conversion, an average pore volume around $0.81 \text{ cm}^3/\text{g}$ should have been attained. The experimental values of ca. $0.40 \text{ cm}^3/\text{g}$ obtained at this conversion suggest that a fraction of toluene is present as a separated phase in the reaction mixture. Nevertheless, the average pore size and pore volume obtained should be suitable for using these nanoparticles in drug delivery systems. In fact, porous

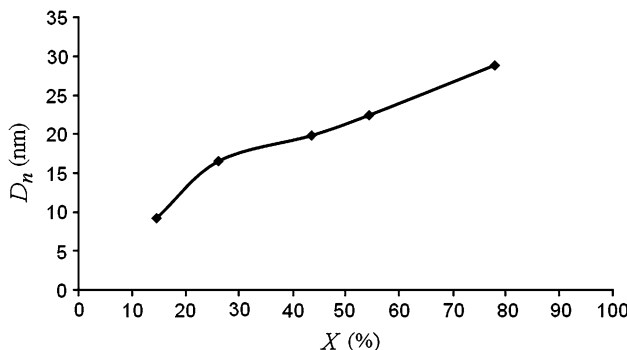
Fig. 3 Histograms obtained from STEM micrographs at different global conversions in run 1: **a** 26.1%, **b** 43.5%, and **c** 77.9%



microparticles with magnetic nanoparticles inside their pores and drugs chemically attached on their surface have been developed for chemotherapy [4–7]. Nanoparticles with pore diameters around 6–8 nm, as the ones obtained here, would allow that

Table 1 Number-average diameter (D_n) and polydispersity index (D_w/D_n) as a function of global conversion for run 1

X (%)	D_n (nm)	D_w/D_n
14.5	9.3	1.2
26.1	16.6	1.2
43.5	19.9	1.2
54.3	22.5	1.2
77.9	28.9	1.1

**Fig. 4** Number-average particle diameter as a function of conversion for run 1**Table 2** Average pore radius (R_{pore}) and pore volume (ϕ) for low, medium, and high global conversions for runs 1 and 2

Run 1			Run 2			σ, R_{pore} (nm)	σ, ϕ (cm^3/g)
X (%)	R_{pore} (nm)	ϕ (cm^3/g)	X (%)	R_{pore} (nm)	ϕ (cm^3/g)		
14.5	2.9	0.32	16.0	3.1	0.35	0.1	0.02
43.5	3.8	0.42	43.1	3.8	0.42	0.0	0.00
77.9	3.4	0.39	76.7	3.8	0.38	0.3	0.01

magnetic nanoparticles, with sizes similar or smaller than those of the pores, to be precipitated or introduced inside the pores. This is important because magnetite nanoparticles smaller than ca. 10 nm are superparamagnetic, which means that they magnetize under a magnetic field, but do not possess remnant magnetization when this field is removed [20]. Furthermore, it is desirable that superparamagnetic nanoparticles to be as close as possible to 10 nm because the well known direct dependence between particle size and saturation magnetization for superparamagnetic nanoparticles [21]. Hence, drug delivery systems with relatively large superparamagnetic nanoparticles inside could be directed more easily by an external magnetic field for reaching the targets inside the human body. Moreover, they will not agglomerate when the magnetic field is removed.

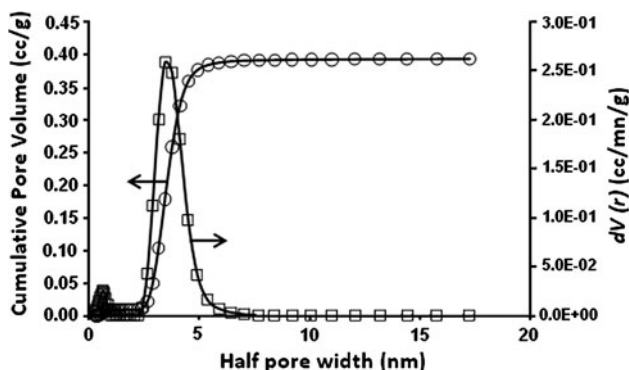


Fig. 5 Graph provided by the automated surface area and pore size analyzer for the final sample of run 1

Table 3 Required and available surfactant in the total mixture at medium and high conversions for run 1

X (%)	$N_p \times 10^{-16}$ (mL ⁻¹ water)	SDS required (g)	SDS available (g)
43.5	3.6	3.51	3.52
77.9	2.3	4.10	3.14

An estimation of the surfactant required for covering all particles in the reaction mixture in a saturated monolayer at 43.5 and 77.9% global conversions, allows us to explain the decrease in particle size polydispersity with global conversion at the latter stages of the polymerization. As a first approximation, calculations were carried out considering monomer-free particles, that is, non-swollen particles. D_n determined by STEM, polymer concentrations [P] in the latex, density of porous polymeric particles (ρ_{por}) calculated from polystyrene density (1.05 g/mL) [22] and pore volume, were used to calculate particle number density (N_p) using the following equation:

$$N_p = \frac{6[P]}{\pi \rho_{\text{por}} D_n^3} \quad (3)$$

With N_p values, the total water in the reaction mixture and the area occupied by one SDS molecule in a saturated monolayer on the particle surface (0.5 nm²) [23], the amount of surfactant required for stabilizing all particles at global conversions given above was estimated. The critical micelle concentration of SDS (7 mM) [23] was considered in these calculations. Table 3 shows N_p values along with those of the amount of SDS required and available in the mixture reaction at 43.5 and 77.8% conversions. Data in Table 3 indicate that from around 45% global conversion, the amount of surfactant in the reaction mixture is insufficient for complete stabilization of particles, although they were considered non-swollen particles. As a consequence, even before 45% global conversion, there is not enough surfactant for stabilizing all the monomer-swollen particles, which explains the decrease in N_p above 45% conversion due to particle's coagulation. Coagulation between small and large particles (hetero-coagulation) is a well-known mechanism for narrowing

particle size distribution in emulsion polymerization [24]. Then, the decrease in PDI shown in Table 2 could be due to hetero-coagulation.

Conclusions

Semicontinuous heterophase polymerization at 60 °C of St with DVB as crosslinking agent and toluene as porogen allowed to produce mesoporous polystyrene nanoparticles with mean diameter around 30 nm, pores of 6–8 nm in diameter and pore volumes around 0.40 cm³/g. In spite that the polymerization was not carried out at highly monomer-starved conditions, narrow particle size distribution was obtained. This was ascribed to inter-particle hetero-coagulation at latter stages of polymerization, which arises from a lack of enough surfactant to cover all the particles even before 45% global conversion. This report could be the basis for synthesizing polymeric nanoparticles with low-to-medium porosity containing pores with diameters between 6 and 8 nm, which will permit to precipitate or charge inside them superparamagnetic nanoparticles with relatively high magnetization.

Acknowledgments National Council of Science and Technology (CONACyT) supported this research through grants SEP 2007-84009 and CB-2007-82437. We are grateful to Patricia Siller and Daniel Alvarado for their technical assistance.

References

1. Arshady R (1991) Beaded polymer supports and gels. II. Physico-chemical criteria and functionalization. *J Chromatogr A* 586:199–219
2. Chengyou K, Huihui L, Qing Y, Xiangzheng K (1997) Preparation of porous latex particles by emulsion polymerization. *Korea Polym J* 5:221–227
3. Arayne MS, Sultana N (2006) Porous nanoparticles in drug delivery system. *Pak J Pharm Sci* 19:155–158
4. Tartaj P, Morales MP, Veintemillas-Verdaguer S, González-Carreño T, Serna C (2003) The preparation of magnetic nanoparticles for applications in biomedicine. *J Phys D* 36:R182–R197
5. Roca AG, Costo R, Rebolledo AF, Veintemillas-Verdaguer S, Tartaj P, González-Carreño T, Morales MP, Serna CJ (2009) Progress in the preparation of magnetic nanoparticles for applications in biomedicine. *J Phys D* 42:224002 (11 pp)
6. Berry CC (2009) Progress in functionalization of magnetic nanoparticles for applications in biomedicine. *J Phys D* 42:224003 (9 pp)
7. Pankhurst QA, Thanh NKT, Jones SK, Dobson J (2009) Progress in applications of magnetic nanoparticles in biomedicine. *J Phys D* 42:224001 (15 pp)
8. Kammona O, Dini E, Kiparissides C (2004) Synthesis of porous polymeric nanoparticles for water treatment applications. In: Kreysa (ed) 8th International workshop on polymer reaction engineering. Dechema monographs 138. Wiley-VCH Verlag, Germany, pp 343–347
9. Kim JW, Lee JE, Kim SJ, Lee JS, Ryu JH, Kim J, Han SH, Chang IS, Suh KD (2004) Synthesis of silver/polymer colloidal composites from surface-functional porous polymer microspheres. *Polymer* 45:4741–4747
10. Macintyre FS, Sherrington DC, Tetley L (2006) Synthesis of ultrahigh surface area monodisperse porous polymer nanospheres. *Macromolecules* 39:5381–5384
11. Maillard-Terrier MC, Cazé C (1984) Texture poreuse de copolymères 4-vinylpyridine divinylbenzène. *Eur Polym J* 20:113–118

12. Arshady R, Ledwith A (1983) Suspension polymerization and its application to the preparation of polymer supports. *React Polym* 1:159–174
13. Arshady R (1999) Polymer supports, reagents and catalysts. In: Arshady R (ed) *Microspheres, microcapsules and liposomes*. City Books, London, pp 197–235
14. Arshady R (1999) Microspheres, microcapsules and liposomes: definitions, nomenclature and terminology. In: Arshady R (ed) *Microspheres, microcapsules and liposomes*. City Books, London, pp 55–81
15. Puig JE (1999) Synthesis and applications of nanoparticles via microemulsion polymerization. *Rev Mex Fis* 45:18–20
16. Co CC, de Vries R, Kaler EW (2001) Free radical polymerization in microemulsions. In: Texter J (ed) *Reactions and synthesis in surfactant systems*. Marcel Dekker, New York, pp 455–470
17. Sajjadi S (2007) Nanoparticle formation by monomer-starved semibatch emulsion polymerization. *Langmuir* 23:1018–1024
18. Ledezma R, Treviño ME, Elizalde LE, Mendizábal E, Puig JE, López RG (2007) Semicontinuous heterophase polymerization under monomer starved conditions to prepare nanoparticles with narrow size distribution. *J Polym Sci Pol Chem* 45:1463–1473
19. Duda JT, Jagiello L, Jagiello J, Milewska-Duda J (2007) Complementary study of microporous adsorbentes with DFT and LBET. *Appl Surf Sci* 253:5616–5621
20. Cornell RM, Schwertmann U (1996) The iron oxides: structure, properties, reactions, occurrence and uses. Wiley-VCH, Weinheim
21. Liz L, López-Quintela MA, Mira J, Rivas J (1994) Preparation of colloidal Fe_3O_4 ultrafine particles in microemulsions. *J Mater Sci* 29:3797–3801
22. Brandrup J, Immergut EH, Grulke EA (1999) *Polymer handbook*. Wiley, Hoboken
23. Ramírez AG, López RG, Tauer K (2004) Studies on semibatch microemulsion polymerization of butyl acrylate: Influence of the potassium peroxodisulfate concentration. *Macromolecules* 37:2738–2747
24. Coen EM, Gilbert RG, Morrison BR, Leube H, Peach S (1998) Modelling particle size distributions and secondary particle formation in emulsion polymerization. *Polymer* 39:7099–7112